Surgical and Radiologic Anatomy (2019) 41:529–534
https://doi.org/10.1007/s00276-019-02184-0

ORIGINAL ARTICLE

The diaphragma sellae, diaphragm opening, and subdiaphragmatic cistern: an anatomical study using magnetic resonance imaging

Satoshi Tsutsumi[1] · **Hideo Ono**[2] · **Yukimasa Yasumoto**[1] · **Hisato Ishii**[1]

Received: 30 October 2018 / Accepted: 10 January 2019 / Published online: 17 January 2019

Abstract

Purpose Few studies have explored the detailed morphology of the diaphragma sellae (DS), diaphragm opening (DO) or stoma, and subdiaphragmatic cistern (SDC) using neuroimages. The aim of the present study was to characterize these structures using magnetic resonance imaging.

Methods Thin-sliced, sagittal and coronal T2-weighted imaging was performed for a total of 84 outpatients.

Results The DS, DO, SDC, and relevant structures were consistently delineated in all patients. In 66% of patients, all three structures appeared to be highly variable, and were classifiable as six distinct morphological types. In 4% of patients, the DS presented as a complete sheet lacking a discernible DO. In addition, 30% of the patients presented with undiscernible SDCs. In the coronal sections of 11% of patients, the pituitary glands extended laterally, reaching or extending beyond the center line on the sectional image of the cavernous internal carotid artery.

Conclusions Thin-sliced, sagittal, and coronal T2-weighted sequences are useful for delineating the DS, DO, and SDC. Morphological variation of these structures among individuals may considerably influence the direction of pituitary tumor expansion.

Keywords Diaphragm · Diaphragmatic stoma · Subdiaphragmatic · MRI

Introduction

The medial part of the superior wall of the cavernous sinus is known as the diaphragma sellae (DS), and covers the sella turcica. The superior wall of the cavernous sinus and the DS are continuous structures formed by two layers: a smooth superficial dural layer and a thin, less-defined, deeper layer [2, 19, 24]. The DS is thought to develop from the plica ventralis encephali, a distinct primitive mesenchymal fold, at 9–10 weeks of gestation [4]. The pituitary stalk passes through a central opening in the DS that has variable size and shape [1, 2, 10, 11, 13, 14, 16, 19–21, 25, 26]. The posterior marginal quadrant of the DS is mainly supplied by the inferior hypophyseal artery, the right and left marginal quadrants by the tributaries of the intracavernous portion of the internal carotid artery, and the anterior marginal quadrant by the anterior capsular arteries [17]. An inconsistent but distinct small subarachnoid space, the subdiaphragmatic cistern (SDC), extends between the upper surface of the pituitary gland and the lower surface of the DS [8]. The SDC communicates with the suprasellar cistern though the diaphragm opening (DO) or stoma. The size and shape of the DS and SDC may be influenced by the morphology of the pituitary gland, sella turcica, and the arachnoids encircling the pituitary stalk [5, 9, 23].

However, to our knowledge, few studies have used neuroimaging to document the detailed morphology of the DS, DO, and SDC [6, 8, 12, 18]. The aim of the present study was to characterize these structures using thin-sliced, T2-weighted magnetic resonance (MR) imaging.

✉ Satoshi Tsutsumi
shotaro@juntendo-urayasu.jp

[1] Department of Neurological Surgery, Juntendo University Urayasu Hospital, 2-1-1 Tomioka, Urayasu 279-0021, Chiba, Japan

[2] Division of Radiological Technology, Medical Satellite Yaesu Clinic, Tokyo, Japan

Materials and methods

The present study included a sample of 84 outpatients treated at our hospital between September 2011 and September 2014. These patients suffered from headaches, dizziness, vertigo, tinnitus, hearing disturbances, hemisensory disturbances, and seizures. The sample comprised 39 men and 45 women with a mean age of 53.6 years (range 12–81 years). Initial examinations with axial T1- and T2-weighted images, T2-gradient echo, fluid-attenuated inversion recovery, and diffusion-weighted sequences confirmed that none of the patients had experienced previous intracranial hemorrhage, brain tumors, hypertrophic pachymeningitis, traumatic brain injury, hydrocephalus, cysts, or lesions in the sellar, parasellar, and suprasellar regions. These patients underwent examination with thin-sliced, sagittal and coronal T2-weighted sequences involving the pituitary gland and sellar, parasellar, and suprasellar regions. For each T2 sequence, the following parameters were used: repetition time, 3500.0 ms; echo time, 90.0 ms; slice thickness, 2.0 mm; interslice gap, 0 mm; matrix, 300 × 189; field-of-view, 200 mm × 200 mm; flip angle, 90°; and scan duration, 2 min 40 s. All sequences were obtained using a 3.0T MR scanner (Achieva R2.6; Philips Medical Systems; Best, The Netherlands). Imaging data were transferred to a workstation (Virtual Place Lexus64, 64 edition; AZE; Tokyo, Japan) and analyzed independently by two of the authors (S.T. and H.I.).

The study was performed in accordance with our institution's guidelines for human research. Written informed consent was obtained from all patients prior to their participation.

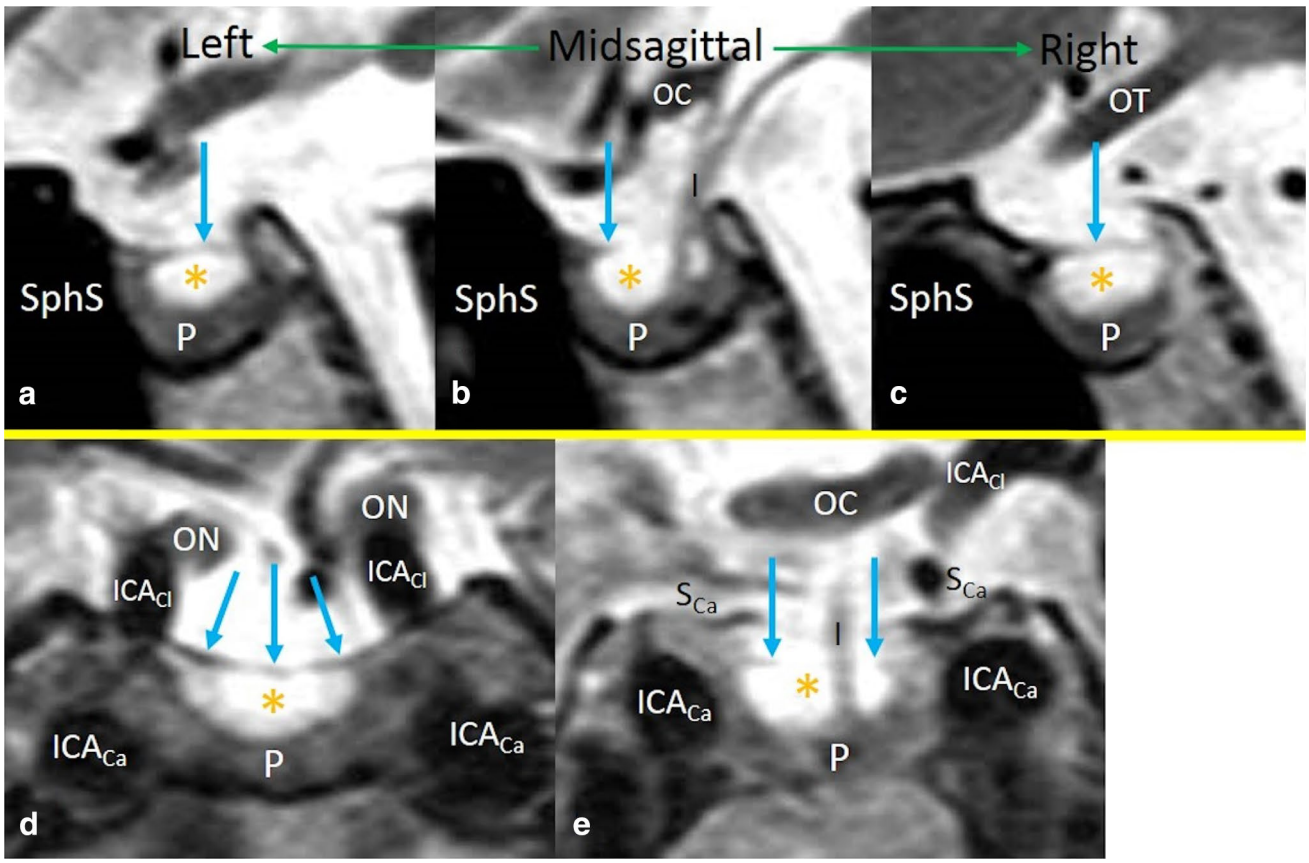

Fig. 1 Sagittal (**a–c**) and coronal (**d, e**) T2-weighted magnetic resonance images showing the diaphragma sellae, subdiaphragmatic cistern, diaphragm opening, and relevant structures. ***a*** and ***c*** are left and right contiguous images of the midsagittal image (**b**), respectively. *I* infundibulum, ICA_{Ca} cavernous portion of the internal carotid artery, ICA_{Cl} clinoid portion of the internal carotid artery, *OC* optic chiasm, *ON* optic nerve, *P* pituitary gland, S_{Ca} superior wall of the cavernous sinus, *SphS* sphenoid sinus, *arrow* diaphragma sellae, *asterisk* subdiaphragmatic cistern

Results

In all 84 patients, the DS, DO, SDC, and relevant structures were consistently delineated on both the sagittal and coronal T2-weighted sequences (Fig. 1). In 56 patients (66%), the structures of the DS, DO, and SDC appeared to be highly variable; even DS thickness showed considerable variability. These structures could be classified into six distinct morphological types, from *Type a* to *Type f*. *Type a* was characterized by bilateral identification of the DS, SDC, and margins of the DO, and occurred in 12 of the 84 patients (14%). *Type b* was characterized by unilateral identification of the DS, SDC, and margin of the DO, and occurred in 17 patients (20%). *Type c*, characterized by unilateral identification of the DS as a complete sheet lacking a discernible DO or SDC, was observed in 1 patient (1%). *Type d*, characterized by a bilateral hypoplastic DS and unilateral identification of the SDC, occurred in 13 patients (15%). *Type e*, characterized by bilateral identification of the DS and SDC, and dilated, peri-pituitary cerebrospinal fluid (CSF)-filled spaces that communicated with the suprasellar cistern, was seen in 8 patients (10%). *Type f*, characterized by bilateral identification of the DS, SDC, and margins of the DO, with a dilated sella turcica and flattened pituitary gland, was seen in 5 patients (6%) (Fig. 2). In three of the 84 patients (4%), the DS appeared to be a continuous sheet without a discernible diaphragm opening (Fig. 3). In contrast, 25 of the 84 patients (30%) presented with undiscernible SDCs of two different types. The first of these, accompanied by a complete or near-complete DS, was found in 9 (11%) (Fig. 4a), while the latter type exhibited a hypoplastic DS and was found in 16 patients (19%) (Fig. 4b). These results are summarized in Table 1.

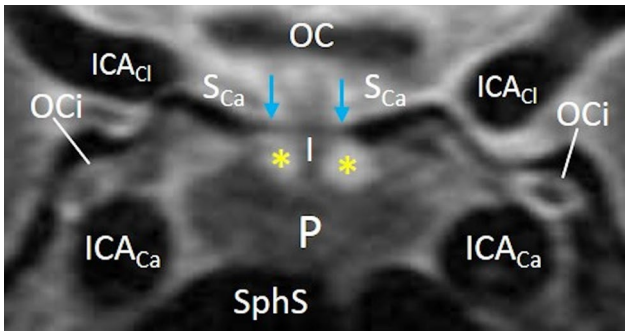

Fig. 3 Coronal T2-weighted magnetic resonance image showing bilaterally complete diaphragma sellae and subdiaphragmatic cistern with undiscernible diaphragm opening

Coronal sections revealed that the pituitary gland extended laterally in 9 patients (11%), reaching or extending beyond the center line on the sectional image of the cavernous internal carotid artery, unilaterally or bilaterally (Fig. 5).

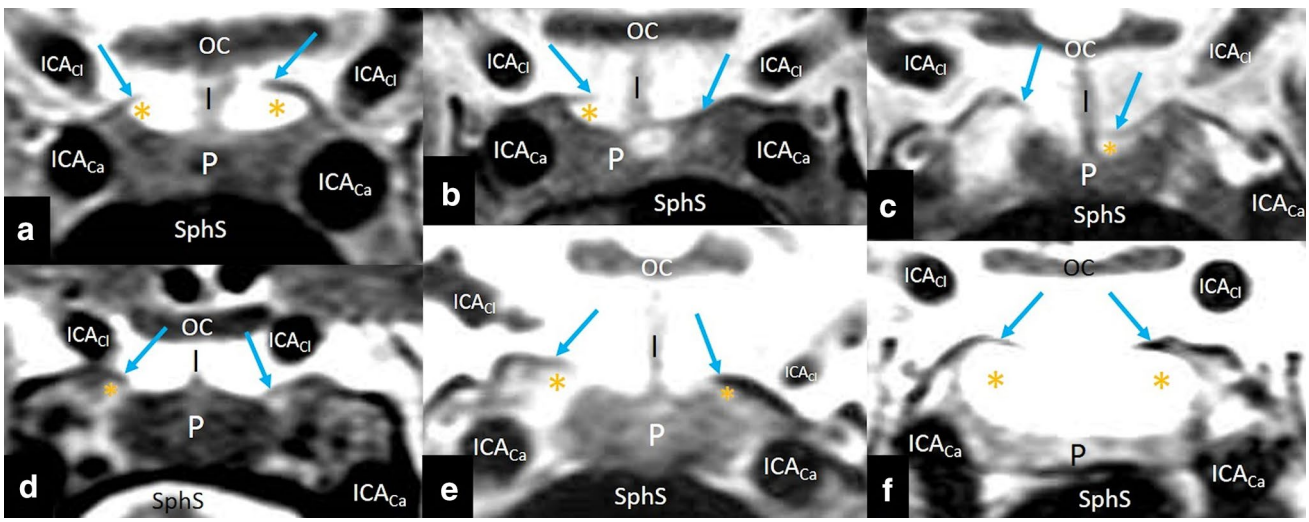

Fig. 2 **a**–**f** Coronal T2-weighted magnetic resonance images of different patients showing variable morphologies of the diaphragma sellae (DS), diaphragm opening (DO), and subdiaphragmatic cistern (SDC). Type a: bilateral identification of the DS, SDC, and margins of the DO; Type b: unilateral identification of the DS, SDC, and margin of the DO; Type c: unilateral identification of the DS as a complete sheet lacking discernible DO and the SDC; Type d: bilateral hypoplastic DS with unilateral identification of the SDC; Type e: bilateral identification of the DS and SDC, and dilated, peri-pituitary cerebrospinal fluid-filled spaces communicating with the suprasellar cistern; Type f: bilateral identification of the DS, SDC, and margins of the DO, with dilated sella turcica and flattened pituitary gland

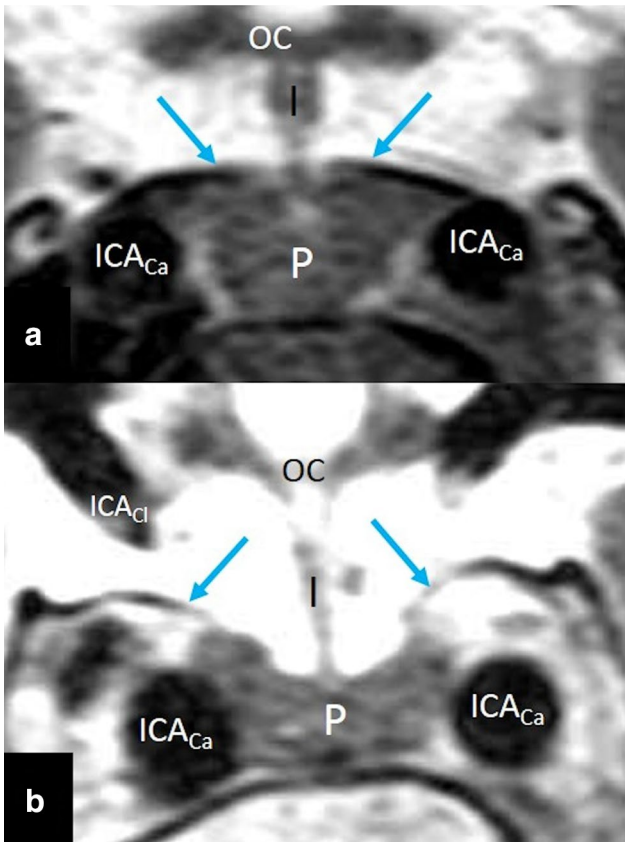

Fig. 4 **a, b** Coronal T2-weighted magnetic resonance images of different patients showing two types of undiscernible subdiaphragmatic cisterns

Table 1 Summary of morphological information for the 84 patients

	Number
Variable DS, DO, and SDC	
Type	
a	12 (14%)
b	17 (20%)
c	1 (1%)
d	13 (15%)
e	8 (10%)
f	5 (6%)
Complete DS	3 (4%)
Undiscernible SDC	
a	9 (11%)
b	16 (19%)
Total	84 (100%)

DO diaphragm opening, DS diaphragma sellae, SDC subdiaphragmatic cistern

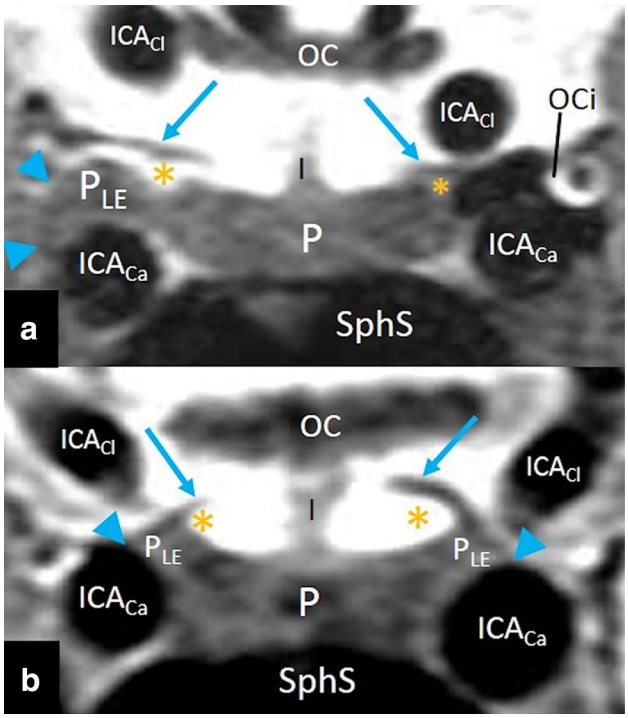

Fig. 5 Coronal T2-weighted magnetic resonance images of different patients showing unilateral (**a**) and bilateral (**b**) lateral extensions of the pituitary gland reaching (**b**) or beyond (**a**) the center line on sectional images of the cavernous internal carotid artery. P_{LE} lateral extension of the pituitary gland, *arrowhead* lateral margin of the pituitary gland

Discussion

In the present study using MR imaging, the DS, DO, SDC, and relevant structures were consistently delineated and showed highly variable morphology which could be classified into six types. Thirty percent of the patients presented with undiscernible SDCs. Eight patients presented with dilated, peri-pituitary CSF-filled spaces communicating with the suprasellar cistern. These spaces were thought to correspond to the spaces identified between the pituitary gland and cavernous internal carotid in cadaveric specimens, and could influence the direction of pituitary tumor extension [3]. Furthermore, in 11% of patients, the pituitary glands extended laterally beyond the midline on the sectional image of the cavernous internal carotid artery. In a previous study using cadaveric specimens, lateral extension of the normal pituitary gland into the cavernous sinus was encountered in 29% of subjects [7]. This finding is critical for assessments of pituitary adenomas with invasion into the cavernous sinus, because in some cases this lateral extension of the normal pituitary gland may be mistaken for lateral tumor invasion into the cavernous sinus [15].

Thin-sliced, sagittal and coronal T2-weighted sequences were acquired for the present investigation, yielding

consistent delineation of the DS, DO, and SDC. Supporting a previous study, our results confirm the utility of high-resolution T2-weighted imaging for detecting the fine dural structures of the sellar and parasellar regions [22].

There are limitations to the present study. Our investigation applied a retrospective analysis to a relatively small and heterogenous sample. Participants were not randomly assigned to our sample; therefore, we did not use statistical analyses. Finally, the DS, DO, and SDC were delineated only on the sagittal and coronal planes, and were not assessed as three-dimensional architectures. However, we nonetheless consider these findings helpful for improving our understanding of both *in vivo* anatomy of the DS, DO, and SDC, and the potential directions of pituitary tumor extension.

Conclusions

Thin-sliced, sagittal and coronal T2-weighted sequences are useful for delineating the SDC and DS. The morphology of these structures exhibits considerable inter- and intra-individual variability that probably influences the direction of pituitary tumor extension.

Acknowledgements This work was not supported by grant funding.

Author contributions Satoshi Tsutsumi developed the study design. Hisato Ishii and Yukimasa Yasumoto collected the imaging data. Hideo Ono and Hisato Ishii analyzed the imaging data. Satoshi Tsutsumi wrote the manuscript.

Compliance with ethical standards

Conflict of interest The authors have no conflicts of interest concerning the materials or methods used in this study, or the findings presented in this paper.

References

1. Abuzayed B, Tanriöver N, Ozlen F, Gazioğlu N, Ulu MO, Eraslan B, Akar Z (2009) Endoscopic endonasal transsphenoidal approach to the sellar region. Results of endoscopic dissection on 30 cadavers. Turk Neurosurg 19:237–244
2. Campero A, Martins C, Yasuda A, Rhoton AL Jr (2008) Microsurgical anatomy of the diaphragma sellae and its role in direction the pattern of growth of pituitary adenomas. Neurosurgery 62:717–723
3. Cebula H, Kurbanov A, Zimmer LA, Poczos P, Leach JL, De Battista JC, Froelich S, Theodosopoulos PV, Keller JT (2014) Endoscopic endonasal variability in the anatomy of the internal carotid artery. World Neurosurg 82:e759–e764
4. Cho KH, Rodríguez-Vázquez JF, Han EH, Verdugo-López S, Murakami G, Cho BH (2010) Human primitive meninges in and around the mesencephalic flexure and particularly their topographical relation to cranial nerves. Ann Anat 192:322–328
5. Ciappetta P, Pescatori L (2017) Anatomic dissection of arachnoid membranes encircling the pituitary stalk on fresh, non-formalin-fixed specimens: anatomoradiologic correlations and clinical applications in craniopharyngioma surgery. World Neurosurg 108:479–490
6. Daniels DL, Pojunas KW, Kilgore DP, Pech P, Meyer GA, Williams AL, Haughton VM (1986) MR of the diaphragms sellae. AJNR Am J Neuroradiol 7:765–769
7. Destrieux C, Kakou MK, Velut S, Lefrancq T, Jan M (1998) Microanatomy of the hypophyseal fossa boundaries. J Neurosurg 88:743–752
8. Di leva A, Tschabitscher M, Matula C, Komatsu F, Komatsu M, Colombo G, Sherif C, Galzio RJ (2012) The subdiaphragmatic cistern: historic and radioanatomic findings. Acta Neurochir (Wien) 154:667–674
9. Doraiswamy PM, Potts JM, Axelson DA, Husain MM, Lurie SN, Na C, Eacalona PR, McDonald WM, Figiel GS, Ellinwood EH Jr et al (1992) MR assessment of pituitary gland morphology in healthy volunteers: age- and gender-related differences. AJNR Am J Neuroradiol 13:1295–1299
10. Ferreri AJ, Garrido SA, Markarian MG, Yañez A (1992) Relationship between the development of diaphragma sellae and morphology of the sella turcica and its content. Surg Radiol Anat 14:233–239
11. Guinto Balanzar G, Abdo M, Mercado M, Guinto P, Nishimura E, Arechiga N (2011) Diaphragma sellae: a surgical reference for transsphenoidal resection of pituitary macroadenomas. World Neurosurg 75:286–293
12. Guitelman M, Garcia Basavilbaso N, Vitale M, Chervin A, Katz D, Miragaya K, Herrera J, Cornalo D, Servidio M, Boero L, Manavela M, Danilowicz K, Alfieri A, Stalldecker G, Glerean M, Fainstein Day P, Ballarino C, Mallea Gil MS, Rogozinski A (2013) Primary empty sella (PES): a review of 175 cases. Pituitary 16:270–274
13. Gulsen S, Dinc AH, Unal M, Cantürk N, Altinors N (2010) Characterization of the anatomic location of the pituitary stalk and its relationship to the dorsum sellae, tuberculum sellae and chiasmatic cistern. J Korean Neurosurg Soc 47:169–173
14. Ju KS, Bae HG, Park HK, Chang JC, Choi SK, Sim KB (2010) Morphometric study of the Korean adult pituitary glands and the diaphragma sellae. J Korean Neurosurg Soc 47:42–47
15. Knosp E, Steiner E, Kitz K, Matula C (1993) Pituitary adenomas with invasion of the cavernous sinus space: a magnetic resonance imaging classification compared with surgical findings. Neurosurgery 33:610–618
16. Kursat E, Yilmazlar S, Aker S, Aksoy K, Oyguch H (2008) Comparison of lateral and superior walls of the pituitary fossa with clinical emphasis on pituitary adenoma extension: cadaveric-anatomic study. Neurosurg Rev 31:91–98
17. Lee KF, Parke W, Lin SR, Choi HY, Schatz NJ (1978) The vasculature of the diaphragma sellae. A postmortem injection study. Neuroradiology 16:281–283
18. Nomura M, Tachibana O, Yamashima T, Yamashita J, Suzuki M (2002) MRI evaluation of the diaphragmal opening: using MRI parallel to the transsphenoidal surgical approach. J Clin Neurosci 9:175–177
19. Renn WH, Rhoton AL Jr (1975) Microsurgical anatomy of the sellar region. J Neurosurg 43:288–298
20. Sage MR, Blumbergs PC, Fowler GW (1982) The diaphragma sellae: its relationship to normal sellar variations in frontal radiographic projections. Radiology 145:699–701
21. Sage MR, Blumbergs PC, Mulligan BP, Fowler GW (1982) The diaphragma sellae: its relationship to the configuration of the pituitary gland. Radiology 145:703–708
22. Thines L, Lee SK, Dehdashti AR, Agid R, Willinsky RA, Wallace CM, Terbrugge KG (2009) Direct imaging of the distal dural ring

and paraclinoid internal carotid artery aneurysms with high-resolution T2 turbo-spin echo technique at 3-T magnetic resonance imaging. Neurosurgery 64:1059–1064
23. Tsunoda A, Okuda O, Sato K (1997) HR height of the pituitary gland as a function of age and sex: especially physiological hypertrophy in adolescence and in climacterium. AJNR Am J Neuroradiol 81:914–920
24. Umansky F, Valarezo A, Elidan J (1994) The superior wall of the cavernous sinus: a microanatomical study. J Neurosurg 81:914–920
25. Won HS, Han SH, Oh CS, Lee JI, Chung IH, Kim SH (2010) Topographic variations of the optic chiasm and the foramen diaphragma sellae. Surg Radiol Anat 32:653–657
26. Yohannan DG, Krishnapillai R, Suresh R, Ramnarayan S (2015) A morphometric study of diaphragma sellae and delineation of its relation to optic neural pathways through computer aided superimposition. Anat Res Int 618042